

Chap. 12.

¹¹I. P. Ipatova, A. A. Maradudin, and R. F. Wallis, *Phys. Rev.* **155**, 882 (1967).

¹²G. Dolling, H. G. Smith, R. M. Nicklow, P. R. Vijayaraghavan, and M. K. Wilkinson, *Phys. Rev.* **168**, 970 (1968).

¹³E. Burstein, F. A. Johnson, and R. Loudon, *Phys. Rev.* **139**, 1239 (1965).

¹⁴R. Stolen and K. Dransfield, *Phys. Rev.* **139**, 1295 (1965).

¹⁵A. Hadni, in *Far Infrared Properties of Solids*, edited by S. S. Mitra and S. Nudelman (Plenum, New York, 1970), p. 561.

¹⁶R. P. Lowndes and D. H. Martin, *Proc. Roy. Soc. (London)* **308**, 473 (1969).

¹⁷S. S. Jaswal and J. R. Hardy, in *Localized Excitations*

in *Solids*, edited by R. F. Wallis (Plenum, New York, 1968), p. 643.

¹⁸R. F. Caldwell and M. V. Klein, *Phys. Rev.* **158**, 851 (1967). This technique amounted to convoluting the theoretical points evenly spaced in wave number, with a symmetrical triangular function. A further improvement could be obtained by using a function which represents a least-squares fit to some order of polynomial.

¹⁹M. Born and K. Huang, *Dynamical Theory of Crystal Lattices* (Clarendon, London, 1968), p. 26.

²⁰The manifestation of this coupling rule in two-phonon difference absorption measurements led Stolen and Dransfield (Ref. 14) to state that longitudinal and transverse modes do not combine at all, whereas this is true only in a few cases.

²¹J. E. Eldridge, *Phys. Rev. B* (to be published).

PHYSICAL REVIEW B

VOLUME 6, NUMBER 4

15 AUGUST 1972

Energy-Band Structure of SrTiO₃ from a Self-Consistent-Field Tight-Binding Calculation*

Thomas F. Soules,[†] Edward J. Kelly, and David M. Vaught[‡]
Department of Chemistry, Purdue University, Lafayette, Indiana 47907

and

James W. Richardson
Department of Chemistry, Purdue University, Lafayette, Indiana 47907
and Philips Research Laboratories, Eindhoven, The Netherlands
 (Received 5 November 1971)

Energy bands of SrTiO₃ have been computed *ab initio* using a nonrelativistic self-consistent-field (SCF) procedure based upon the linear-combination-of-atomic-orbitals or tight-binding formalism. A slightly extended multicentered-atomic-orbital basis was used and integrals over them were evaluated in keeping with the Hartree-Fock-Roothaan procedures. Three- and four-centered integrals were treated by previously justified numerical approximations. Results are in good agreement with experimental evidence for the ordering and widths of the valence and conduction bands. A 12.1-eV band gap was obtained, however, from the ground-state SCF results. Consideration of various energy terms and comparison with an independent SCF calculation on the isolated TiO₆⁸ cluster confirm Šimánek and Šroubek's earlier criticism of Kahn and Leyendecker's semiempirical model and suggest significant hole-particle correlation in the electronically excited states of the crystal. Though by a less rigorous analysis, the Sr orbital interactions are judged not to perturb the features of these results.

I. INTRODUCTION

Over the past several years, numerous physical properties of SrTiO₃ and similar transition-metal oxides have been measured with recent interpretations of the electronic properties of SrTiO₃ based on the semiempirical band structure of Kahn and Leyendecker.^{1,2} Their calculated results were in good agreement with the experimental data then available although some discrepancies have since appeared.^{3,4}

Kahn and Leyendecker used an adjustable ionic model to represent the lattice-crystal-field potential. A completely ionic model predicts an energy gap of 17 eV separating the oxide 2*p* valence orbitals from the vacant titanium 3*d* orbitals. Their innovation was to attribute the observed

absorption edge at 3.2 eV to a departure from complete ionicity in the titanium-oxygen bond. Šimánek and Šroubek⁵ correctly criticized their implementation, however, since it neglects changes in the oxide and titanium ionization potentials concomitant with a transfer of charge from the oxygen to titanium atoms. These effects were estimated and found approximately to cancel the effect of the change in Madelung potential at the titanium and oxygen sites. Alternatively, then, to explain the apparent reduction in band gap, Šimánek and Šroubek propose a Heitler-London model for the excited state of the crystal in which the hole and electron are associated with neighboring oxygen and titanium ions, respectively. The transition energy is reduced by large hole-electron interaction and polarization effects on the surrounding

lattice ions. As Fowler⁶ later remarked this amounts to postulating an excitonic excited state.

More recently Mattheiss^{7,8} used a nonrelativistic augmented-plane-wave (APW) method to compute the band structure of ReO_3 , which is structurally and electronically related to SrTiO_3 although it contains one additional electron per unit cell in the conduction band. Mattheiss included corrections to the usual muffin-tin potential and obtained solutions at symmetry points in the Brillouin zone. An arbitrary lowering of the Re $5d$ orbitals relative to the oxygen $2p$'s was then invoked to reduce the band gap sufficiently to obtain agreement with his interpretation of the optical reflectance spectrum.

We have carried out a linear-combination-of-atomic-orbitals (LCAO) or tight-binding calculation of the band structure of SrTiO_3 in which very few significant approximations were made. Because of the obvious numerical difficulties encountered in any completely *ab initio* calculation, previous applications of this method have involved a wide variety of approximations in the Hartree-Fock Hamiltonian. Our calculation was motivated by the realization that many important terms in the expressions for the matrix elements of that operator can be identified with those arising in a Hartree-Fock-Roothaan LCAO treatment of clusters like $(\text{NiF}_6^{-4})^9$ and $(\text{TiO}_6^{-8})^{10}$. Previously written programs for those calculations could therefore be incorporated in band-structure calculations on crystals like SrTiO_3 , so that all nearest-neighbor interactions are evaluated in a more accurate manner. Since it has been shown that different results are obtained with different methods of approximating the Hartree-Fock potential,¹¹ it is important to obtain solutions from calculations in which this potential is treated as accurately as possible to increase confidence that the results reflect the Hartree-Fock approximation and not the particular model potential. Also, in the band-structure calculations presented here, we have achieved a self-consistent solution. The rarity of results from calculations which have been carried to convergence (together with the known sensitivity of the crystal Madelung potential at the titanium and oxygen atom sites to the degree of ionicity¹) make it important to study the effect of achieving self-consistency.

It has been claimed by Fowler⁶ that a Hartree-Fock band calculation should give an energy gap which is larger than the experimental one because the Hartree-Fock approximation neglects the effects of electronic correlation. Previous calculations on rare-gas solids and alkali halides are in agreement with Fowler's prediction.^{12,13} In SrTiO_3 , we obtain a direct band gap of 12 eV, almost four times the experimental optical-absorp-

tion edge which occurs at 3.2 eV.¹⁴ A consideration of configuration interaction among band-to-band excited configurations and a comparison with the excited-state energies of charge-transfer transitions in the isolated TiO_6^{-8} cluster suggest that correlation effects, including a large hole-electron interaction and polarization of the surrounding electronic charge distribution, will reduce the Hartree-Fock band gap by the right amount.

In Sec. II, we briefly sketch the LCAO-SCF (self-consistent-field) method as applied here. In Sec. III, we present the computed ground-state band structure and compare our results with the existing experimental data and with previous crystal and cluster calculations. In Sec. IV, effects arising from the higher-energy $4s$ and $4p$ atomic orbitals of titanium and the $5s$ and $5p$ orbitals of the strontium atoms are investigated. A possible explanation of the optical-absorption edge occurring at 3.2 eV is discussed in Sec. V.

II. METHOD

The LCAO or tight-binding method has previously been used mainly for qualitative purposes. It has been shown, however, that even with a minimal atomic-orbital basis it is capable of giving energy bands in very good agreement with those obtained by a modified-plane-wave expansion.¹⁵⁻¹⁹ The success of the method even in the case of lithium and sodium crystals where the conduction-band electrons behave more like free particles than ones associated with individual atomic orbitals suggests that it would certainly be applicable to the study of the valence and conduction bands of largely ionic crystals.

Briefly, strontium titanate has the cubic perovskite structure. The crystal unit cell is shown in Fig. 1 and the appropriate Brillouin zone is shown in Fig. 2 where the standard notation of Bouckaert, Smoluchowski and Wigner²⁰ is used to designate the various symmetry points and lines.

Wave Functions

The LCAO or tight-binding, closed-shell, ground-state wave function is constructed as an antisymmetrized product of one-electron functions, each of which occurs with both spin functions and is taken to be of the form

$$\phi_{l\vec{k}}(\vec{r}) = \sum_l C_l(\nu\vec{k}) \psi_{l\vec{k}}(\vec{r}), \quad (1)$$

where the partially normalized l th Bloch function for a crystal of N cells is

$$\psi_{l\vec{k}}(\vec{r}) = N^{-1/2} \sum_{\vec{q}} \chi_l(\vec{r} - \vec{R}_q - \vec{\rho}_l) e^{i\vec{k} \cdot (\vec{R}_q + \vec{\rho}_l)}. \quad (2)$$

$\chi_l(\vec{r} - \vec{R}_q - \vec{\rho}_l)$ is an atomic orbital (AO) of titanium ($\vec{\rho}_l = 0$), strontium ($\vec{\rho}_l = \frac{1}{2} \hat{x} + \frac{1}{2} \hat{y} + \frac{1}{2} \hat{z}$), or one of the oxygens ($\vec{\rho}_l = \frac{1}{2} \hat{x}$ or $\frac{1}{2} \hat{y}$ or $\frac{1}{2} \hat{z}$), where \hat{x} , \hat{y} , and

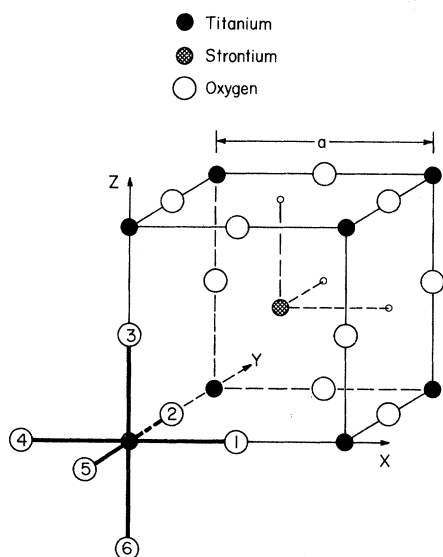


FIG. 1. Structure of SrTiO₃, showing coordination of oxygens about Ti and Sr.

\hat{z} are the basis vectors of the lattice and \vec{R}_q is the lattice vector. The one-electron orbitals ϕ are designated by the wave vector \vec{k} in the first Brillouin zone; ν distinguishes orbitals belonging to the same \vec{k} .

It is convenient to define a frozen-core or "inner"-shell approximation. Theoretically, an improper treatment of the inner-shell electrons has many serious implications. For instance, complete orthogonality among all occupied orbitals should be maintained. Once this is instituted there is no practical advantage to giving the inner shells any special treatment in a numerically exact calculation. We shall, however, designate the Ti 1s, 2s, 2p and O 1s orbitals as inner-shell orbitals

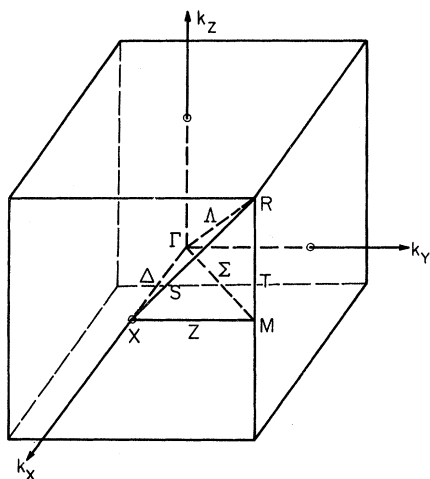


FIG. 2. First Brillouin zone, showing symmetry lines.

which retain their free-ion character.²¹ Hence they are maintained orthogonal to valence shell orbitals on the same center but their nonorthogonality to orbitals on all other centers is neglected.

This approximation amounts to limiting the sum over l in Eq. (1) to $\psi_{l\vec{k}}$ constructed from valence shell AO's or from individual inner-shell AO's, respectively. The subsequent variational calculation is thus restricted to the valence shell orbitals only.

Of the various possible analytical bases, the multicenter Slater-type basis has proved to be accurate and reliable in cluster calculations.⁹ Table I lists parameters for all AO's used. This basis features double- ζ Ti 3d and oxide 2p functions. The former gives a best fit to Watson's Hartree-Fock solution for Ti⁺³.²² The latter was chosen by other criteria mentioned below and is the same

TABLE I. Atomic-orbital basis parameters (Ti-O distance = 3.685 a. u.; for all Sr bases, $\xi_{3d} = 7.5754$).

STO basis		Atomic-orbital coefficients			
nl	ξ_n	$4s(\text{Ti})$	$3s(\text{Ti})$	$2s(\text{Ti})$	$1s(\text{Ti})$
1s (Ti)	21.4409	-0.069 143	0.140 170	-0.329 755	1.000 000
2s (Ti)	7.6883	0.258 801	-0.515 756	1.052 966	...
3s (Ti)	3.6777	-0.623 792	1.113 720
6s (Ti)	3.0600	1.146 527
		$4p(\text{Ti})$	$3p(\text{Ti})$	$2p(\text{Ti})$	
2p (Ti)	9.0324	0.173 131	-0.287 406	1.000 000	
3p (Ti)	3.3679	-0.679 814	1.040 482	...	
6p (Ti)	3.0600	1.194 613	
		$3d(\text{Ti})$			
$3d_i(\text{Ti})$	4.5500	0.457 836			
$3d_o(\text{Ti})$	2.0000	0.668 034			
		$2s(\text{O})$	$1s(\text{O})$		
1s (O)	7.7000	-0.213 878	1.000 000		
2s (O)	2.1250	1.022 616	...		
		$2p(\text{O})$			
$2p_i(\text{O})$	4.4380	0.176 704			
$2p_o(\text{O})$	1.6931	0.888 420			
		$4s(\text{Sr})$	$5s(\text{Sr})$	$5s'(\text{Sr})^a$	
1s (Sr)	37.1911	-0.057 253	0.028 458	0.054 557	
2s (Sr)	13.9509	0.214 538	-0.107 146	-0.206 192	
3s (Sr)	7.5546	-0.480 360	-0.245 490	+0.480 928	
4s (Sr)	3.3327	1.072 173	
4s (Sr)	3.3611	...	-0.633 507	-1.383 831	
5s (Sr)	1.8212	...	1.125 623	...	
6s (Sr)	3.0600	1.576 888	
		$4p(\text{Sr})$	$5p(\text{Sr})$	$5p'(\text{Sr})^a$	
2p (Sr)	17.0152	+0.125 309	-0.054 522	-0.147 839	
3p (Sr)	7.3892	-0.357 373	0.157 641	0.440 001	
4p (Sr)	2.9933	1.042 681	
4p (Sr)	2.9830	...	-0.523 964	-1.840 516	
5p (Sr)	1.5000	...	1.082 004	...	
6p (Sr)	3.0600	1.988 831	

^a Contracted 5s and 5p Sr AO's.

function used in the TiO_6^{-8} cluster calculation.¹⁰ It is somewhat less diffuse than the oxide $2p$ function obtained from a variational calculation on MnO by Nagai²³; both are less diffuse than the $2p$ function of Watson.²⁴

Because the spectra of SrTiO_3 , BaTiO_3 , and even TiO_2 are very similar¹⁴ and because the computational procedures used here are based upon the previous cluster SCF work, our most accurate results are based upon the frequently made assumption that the Sr^{+2} ions may be treated as point charges. The validity of this assumption, as well as criteria for choosing the Sr (and Ti $4s$ and $4p$) functions is covered in Sec. IV.

Variational Equations

We use the nonrelativistic Hartree-Fock equation and operator in the forms

$$F(\vec{r})\phi_{\nu\vec{k}}(\vec{r}) = \epsilon(\nu\vec{k})\phi_{\nu\vec{k}}(\vec{r}), \quad (3)$$

$$F(\vec{r}) = H(\vec{r}) + V_C(\vec{r}) - V_X(\vec{r}), \quad (4)$$

where we use Hartree atomic units and have defined

$$H(\vec{r}) = -\frac{1}{2}\nabla^2 - \sum_n Z_n \left| \vec{r} - \vec{R}_n \right|^{-1}. \quad (5)$$

Z_n is the nuclear charge and \vec{R}_n the lattice position of the n th atom. The Coulomb-potential operator is

$$V_C(\vec{r}) = 2 \sum_{\nu', \vec{k}'} \int |\phi_{\nu'\vec{k}'}(\vec{r}')|^2 \left| \vec{r} - \vec{r}' \right|^{-1} d\vec{r}', \quad (6)$$

and the exchange-potential operator, defined by its effect on an arbitrary function $\chi(\vec{r})$, is

$$V_X(\vec{r})\chi(\vec{r}) = \sum_{\nu', \vec{k}'} \phi_{\nu'\vec{k}'}^*(\vec{r}) \int \phi_{\nu'\vec{k}'}^*(\vec{r}') \chi(\vec{r}') \left| \vec{r} - \vec{r}' \right|^{-1} d\vec{r}'. \quad (7)$$

The sums appearing in the Coulomb and exchange operators are over all occupied orbitals. Spin-orbit and other relativistic terms are not considered because these effects are small for SrTiO_3 and could be adequately treated by perturbation theory.

In order to determine the linear variational coefficients $C_i(\nu\vec{k})$ and the energy bands we set up the usual secular determinant arising from the Hartree-Fock-Roothaan equations²⁵

$$\det | \underline{F}(\vec{k}) - \epsilon(\nu\vec{k})\underline{S}(\vec{k}) | = 0 \quad (8)$$

for each value of \vec{k} . The development of the Fock matrix elements

$$[\underline{F}(\vec{k})]_{ii'} = \langle \psi_{i\vec{k}} | F | \psi_{i'\vec{k}} \rangle, \quad (9)$$

where F is the crystal Fock operator of Eq. (4), and the overlap matrix elements

$$[\underline{S}(\vec{k})]_{ii'} = \langle \psi_{i\vec{k}} | \psi_{i'\vec{k}} \rangle \quad (10)$$

have been presented by Mattheiss⁷ and more completely by Honig, Dimmock, and Kleiner.²⁶ In the application here, only nearest-neighbor Ti-O and

O-O interactions are included. Equations (9) and (10) then reduce to

$$[\underline{F}(\vec{k})]_{ii'} = E(l, l') T_r(l, l'; \vec{k}) \quad (11)$$

and

$$[\underline{S}(\vec{k})]_{ii'} = S(l, l') T_r(l, l'; \vec{k}), \quad (12)$$

with T_r being a trigonometric factor defined below,

$$E(l, l') = \langle \chi_l(\vec{r} - \vec{\rho}_l) | F | \chi_{l'}(\vec{r} - \vec{\rho}_{l'}) \rangle, \quad (13)$$

and

$$S(l, l') = \langle \chi_l(\vec{r} - \vec{\rho}_l) | \chi_{l'}(\vec{r} - \vec{\rho}_{l'}) \rangle. \quad (14)$$

The basic overlap, $S(l, l')$, and transfer, $E(l, l')$, integrals are defined over the orbitals of the TiO_3 asymmetric unit (O_1 , O_2 , O_3 and the nearest Ti in Fig. 1). During the course of computation, each χ_l and its associated variational coefficient $C_l(\nu\vec{k})$ was considered to have been multiplied by $(-i)^{p_l}$ and i^{p_l} , respectively, where $p_l = 0$ or 1 for χ_l of even or odd parity. Thereby all matrix elements of Eqs. (11) and (12) become real and, in terms of the original, real basis the trigonometric factors are given by

$$T_r(l, l'; \vec{k}) = [S(l, l')]^{-1} (i)^{p_l} (-i)^{p_{l'}} \sum_{\vec{q}'} e^{i\vec{k} \cdot (\vec{R}_{q'} + \vec{\rho}_{l'} - \vec{\rho}_l)} \times \langle \chi_l(\vec{r} - \vec{\rho}_l) | \chi_{l'}(\vec{r} - \vec{R}_{q'} - \vec{\rho}_{l'}) \rangle, \quad (15)$$

where the sum over \vec{q}' brings in $\chi_{l'}$ which are, at farthest, nearest neighbors of χ_l . Table II includes the symmetrically independent matrix elements and corresponding trigonometric factors thus defined.

Kahn and Leyendecker¹ variously evaluated the transfer integrals in Eq. (13) and Table II according to the semiempirical recipe of Wolfsberg and Helmholz,²⁷ using their deduced degree of ionicity plus crystal potential considerations. Michel-Calendini and Mesnard²⁸ extended a similar semiempirical calculation to BaTiO_3 , modified to estimate the dependence of Ti and O ionization potentials upon the distribution of charge between Ti and O. We have evaluated these matrix elements *ab initio*, as follows, using essentially the same computational procedures as developed for isolated clusters.²¹ We first consider the total electronic charge-density distribution for the crystal

$$\rho_t(\vec{r}) = 2 \sum_{\nu\vec{k}, \text{occ}} \phi_{\nu\vec{k}}^*(\vec{r}) \phi_{\nu\vec{k}}(\vec{r}) = \sum_{l, l'} \rho_{ll'}(\vec{r}), \quad (16)$$

where the sum includes only occupied (occ) band orbitals and where the contribution from all translationally related functions χ_l and $\chi_{l'}$ is

$$\rho_{ll'}(\vec{r}) = \sum_{\vec{q}, \vec{q}'} D(l, l'; \vec{q}' - \vec{q}) \chi_l^*(\vec{r} - \vec{R}_q - \vec{\rho}_l) \times \chi_{l'}(\vec{r} - \vec{R}_{q'} - \vec{\rho}_{l'}), \quad (17)$$

with

$$D(l, l'; \vec{q}' - \vec{q})$$

TABLE II. Distinct elements for the crystal Hartree-Fock-Roothaan equation.

$\chi_i - \chi_{i'}^a$	$T_r(l, l'; k)^b$	$S(l, l')^{c,d}$	$E(l, l')^{d,e}$	$[D^{cl}]_{ll'}^f$
3s -3s	1	1.0	-2.78832	2.09329
-2s ₁	C _x	0.03458	-0.11711	-0.13074
-2px ₁	S _x	-0.09093	0.28680	0.29582
3px -3px	1	1.0	-1.76158	2.05360
-2s ₁	-S _x	0.05119	-0.13564	-0.22367
-2px ₁	C _x	-0.01049	0.24874	0.38063
-2px ₃	C _z	0.02410	-0.05967	-0.07014
3dz ² -3dz ²	1	1.0	0.05717	0.32439
-2s ₃	C _z	0.12882	-0.17628	0.14295
-2pz ₃	S _z	-0.13917	0.15422	-0.73821
3dxy-3dxy	1	1.0	0.28713	0.05265
-2py ₁	S _x	0.08815	-0.08150	0.29711
2s ₁ -2s ₁	1	1.0	-0.97478	1.96550
-2s ₂	C _x C _y	0.00889	-0.03060	0.00243
-2px ₂	-S _x C _y	0.01940	-0.02817	-0.07314
-2py ₂	C _x S _y	-0.01940	0.03105	-0.03422
2px ₁ -2px ₁	1	1.0	-0.30192	1.67578
-2py ₂	S _x S _y	0.03309	-0.03982	0.10522
-2px ₂	C _x C _y	-0.02284	0.01920	0.07740
2py ₁ -2py ₁	1	1.0	-0.27182	1.94533
-2px ₂	S _x S _y	0.03309	-0.03050	-0.19559
2pz ₁ -2pz ₂	C _x C _y	0.01025	-0.02358	-0.02612

^aAO's with numerical subscripts are located on that numbered oxygen; see Fig. 1. Other AO's are located on titanium.

^bTrigonometric factor, defined by Eq. (15). $C_\alpha = 2 \cos \frac{1}{2} k_\alpha a$ and $S_\alpha = \sin \frac{1}{2} k_\alpha a$, where a is the lattice constant.

^cOverlap integrals over AO's associated with the asymmetric unit at $R_q = 0$. See Eq. (14).

^dThese integrals are directly related to the LCAO parameters of Refs. 7 and 26.

^eConverged transfer matrix elements. See Eq. (13). Energies in a. u.

^fDensity matrix elements from converged occupied vectors. See Eq. (21) and associated discussion.

$$= \frac{2}{N} \sum_{\nu \vec{k}, \text{occ}} C_i^*(\nu \vec{k}) C_{i'}(\nu \vec{k}) e^{i \vec{k} \cdot (\vec{R}_q - \vec{R}_q + \vec{\rho}_i - \vec{\rho}_{i'})}. \quad (18)$$

When the LCAO coefficients are replaced by the real coefficients as mentioned above, when each term in the sum over \vec{k} is replaced by the average of all terms associated with the star of that \vec{k} , and when values of $\vec{q} - \vec{q}'$ are consistent with the nearest-neighbor condition, Eq. (18) becomes

$$D(l, l'; \vec{q} - \vec{q}') = \frac{2}{N} \sum_{\nu \vec{k}, \text{occ}} C_i(\nu \vec{k}) C_{i'}(\nu \vec{k}) g(l, l') T_r(l, l'; \vec{k}), \quad (18')$$

where $g(l, l')$ is $\frac{1}{2}$ if (l, l') refers to oxygen functions on two different centers and is unity otherwise. Equations (16) and (18') are now symmetric in l and l' ; the former may be restated as

$$\rho_t(\vec{r}) = \sum_{i \geq i'} \rho_{ii'}(\vec{r}), \quad (16')$$

with the replacement

$$D(l, l'; \vec{q} - \vec{q}') - (2 - \delta_{ll'}) D(l, l'; \vec{q} - \vec{q}'). \quad (19)$$

We divide $\rho_{ii'}(\vec{r})$ into a part, $\rho_{ii'}^{cl}(\vec{r})$, assigned to a TiO₆ cluster about $\vec{R}_q = 0$ and a part, $\rho_{ii'}^{ext}(\vec{r})$, assigned to the rest of the crystal:

$$\rho_{ii'}(\vec{r}) = \rho_{ii'}^{cl}(\vec{r}) + \rho_{ii'}^{ext}(\vec{r}). \quad (20)$$

At this point in the computational scheme $\rho_{ii'}^{ext}(\vec{r})$ is to be represented by a collection of point charges and the ll' element of a cluster density vector to be defined, such that

$$\rho_{ii'}^{cl}(\vec{r}) = [\underline{D}^{cl}]_{ll'} \chi_l(\vec{r} - \vec{\rho}_l) \chi_{l'}(\vec{r} - \vec{\rho}_{l'}). \quad (21)$$

In Eq. (21) and what follows in this section, the basis and range of l and l' are extended to encompass also the functions of O₄, O₅, and O₆, which are translationally related to those of O₁, O₂, and O₃, respectively (see Fig. 1).

Three cases arise in relating the elements of \underline{D}^{cl} to the various $D(l, l'; \vec{q}' - \vec{q})$ in Eq. (17). In that equation but with respect to the cluster, $(\vec{R}_q - \vec{\rho}_l)$ and $(\vec{R}_{q'} - \vec{\rho}_{l'})$ may designate sites which occur (a) both within, (b) both without, and (c) one within and the other without. In case (a) $D(l, l'; \vec{q}' - \vec{q})$ is entered into $[\underline{D}^{cl}]_{ll'}$. In case (c) the contribution has been neglected unless one site is a cluster O and the other is an extra-cluster, nearest-neighbor Ti or O. In the former event, the neglect is warranted by the smallness of the overlap distribution it multiplies in Eq. (17). In the latter event, half the amount of charge in that overlap distribution,

$$\frac{1}{2} D(l, l'; \vec{q}' - \vec{q}) \langle \chi_l(\vec{r} - \vec{R}_q - \vec{\rho}_l) | \chi_{l'}(\vec{r} - \vec{R}_{q'} - \vec{\rho}_{l'}) \rangle,$$

is added to $[\underline{D}^{cl}]_{ll}$ or $[\underline{D}^{cl}]_{l'l'}$, depending upon whether χ_l or $\chi_{l'}$, respectively, is associated with the cluster.

Similarly according to the Mulliken gross-atom-population analysis,²⁹ all extra-cluster overlap populations of case (b) are partitioned among the subtended atoms, yielding a net charge to be assigned to each ion outside the cluster, q_{T1} and q_O , when combined with the core charges on those ions.

Now the transfer integrals $E(l, l')$ may be collected into the matrix \underline{E} and stated in the following matrix form:

$$\underline{E} = \underline{H} + \underline{D}^{cl} (\mathcal{J} - \frac{1}{2} \mathcal{K}). \quad (22)$$

The elements of the Coulomb and exchange (super) matrixes \mathcal{J} and \mathcal{K} are defined as usual over all cluster AO's;

$$\mathcal{J}(ll' | mm') = \iint \frac{\chi_l(\vec{r}) \chi_{l'}(\vec{r}) \chi_m(\vec{r}') \chi_{m'}(\vec{r}')}{|\vec{r} - \vec{r}'|} d\vec{r} d\vec{r}', \quad (23)$$

$$\mathcal{K}(l'l' | mm') = \frac{1}{2} \iint \frac{\chi_l(\vec{r})\chi_{l'}(\vec{r}')[\chi_m(\vec{r})\chi_m(\vec{r}') + \chi_{m'}(\vec{r})\chi_m(\vec{r}')] }{|\vec{r} - \vec{r}'|} d\vec{r} d\vec{r}' . \quad (24)$$

The \underline{H} elements are given by

$$[\underline{H}]_{l,l'} = \langle \chi_l | H(\vec{r}) + V_{\text{core}}(\vec{r}) + V_{\text{ext}}(\vec{r}) | \chi_{l'} \rangle, \quad (25)$$

with $H(\vec{r})$ from Eq. (4); also

$$[\underline{V}_{\text{core}}(\vec{r})]_{l,l'} = \sum_{\nu} [2\mathcal{G}(\nu\nu | l'l') - \mathcal{K}(\nu\nu | l'l')], \quad (26)$$

where ν runs over all frozen core orbitals of the TiO_6 cluster. $V_{\text{ext}}(\vec{r})$ arises from the (point) charges outside the cluster; it is found rather constant within the region of the cluster.³⁰ Hence it is adequate to put $\langle \chi_l | V_{\text{ext}} | \chi_l \rangle = V_{\text{ext}}(\text{Ti})$ or $V_{\text{ext}}(\text{O})$ for χ_l on Ti or O, respectively, and

$$\begin{aligned} \langle \chi_l | V_{\text{ext}} | \chi_{l'} \rangle &= \frac{1}{2} S(l, l') [\langle \chi_l | V_{\text{ext}} | \chi_l \rangle \\ &+ \langle \chi_{l'} | V_{\text{ext}} | \chi_{l'} \rangle] \end{aligned} \quad (27)$$

otherwise. Values of $V_{\text{ext}}(\vec{r})$ at the Ti and O sites of the cluster are obtained by subtracting the potential from a point-charge representation of the cluster from the total Madelung potential.³¹ In terms of the lattice constant, a , and in a. u.

$$\begin{aligned} -aV_{\text{ext}}(\text{Ti}) &= 2.8372975q_{\text{Ti}} + 12.2877969q_{\text{O}} \\ &+ 0.8019360q_{\text{Sr}}, \\ -aV_{\text{ext}}(\text{O}) &= 2.0959323q_{\text{Ti}} + 10.6591948q_{\text{O}} \\ &+ 0.5825215q_{\text{Sr}}. \end{aligned}$$

If the integrals in Eqs. (23)–(25) are available, not over the cluster AO's themselves, but alternatively over a symmetry-adapted linear transformation of them, \underline{D}^{cl} may first be transformed to that basis, the contraction $\underline{D}^{cl}(\mathcal{G} - \frac{1}{2}\mathcal{K})$ carried out, and that result transformed back to the AO basis. This procedure was followed here, not only to make use of existing computer programs for the cluster but also to effect considerable computational economies.

Further Numerical Considerations

Of the required integrals appearing in Eqs. (23)–(25) all one- and two-center integrals were obtained exactly. Because of the large amount of computer time required to evaluate all three- and four-center integrals, the former were uniformly approximated using the Mulliken approximation,³² and the latter neglected. These approximations have been extensively investigated in connection with calculations on transition metal clusters.⁹

With respect to electronic spectra, the neglect of non-nearest-neighbor Ti-Ti, Ti-O, and O-O interactions is not so serious an approximation as might first be thought. All titanium AO's through

the 3d are quite localized about that center and do not penetrate significantly beyond the adjacent oxygens. Our oxide functions were designed to reasonably represent behavior within the region of that ion and its nearest neighbors but to be small at greater distances. Thus none of these non-nearest-neighbor interactions should exceed 0.1 eV in magnitude.

In their tight-binding calculations on VO, Norwood and Fry investigated and included up to fourth neighbors in metal 3d-3d and O-O overlap interactions.¹⁹ Most of the former, which arise in the rock-salt structure of VO, do not occur in the perovskite structure. The magnitudes of the remaining ones (except for the 002 xz , xz potential + KE element, which seems inordinately large) are consistent with our approximation. In addition, it is to be recalled, we have *designed* our Ti and O basis functions to minimize further these longer-range interactions. On the other hand, the Sr 5s and 5p functions, which we include later, are considered in Sec. IV.

It should be emphasized that the truly optimum basis for any crystal calculation has yet to be found. Use of free-ion atomic orbitals is more easily defended in representing the interior regions of the ionic constituents of the solid than their long-range behavior. In nonempirical calculations such as this, one may choose a basis in part with an eye toward minimizing the consequences of some purely mathematical complexities. Ionic-type compounds appear particularly suited to this numerical simplification.

Furthermore, causing those interaction elements deemed significant to be computationally related to just those found within a single TiO_6 cluster allowed the use of some existing computer programs. To generalize the methodology to encompass any given additional degree of longer-range interaction is relatively straightforward. In expanding the Fock and overlap elements of the secular equation, Eqs. (9) and (10), additional terms occur in Eqs. (11) and (12) as shown by Mattheiss⁷ and Honig, Dimmock, and Kleiner.²⁶ Each added term again is a product of a structure-determined trigonometric factor and an energy or overlap element connecting two basis functions at the greater separation. The energy elements $E(l, l')$ again might be evaluated by the same basic computational procedure as described above, though conducted in terms of a sufficiently different or larger cluster unit which encompasses the additional interactions. Except appropriately to alter the range of the basis function indices $l'mm'$ and the constituents of

V_{ext} , the formalism following Eq. (15) would appear unchanged.

In Eq. (18'), the summand was first considered to be continuous in \vec{k} and summation replaced by integration. The resulting three-dimensional integration was then done by a numerical-quadrature scheme using seven-point Simpson's rule in each dimension. Values of the $C_i(\nu\vec{k})$ at the 343 required points in \vec{k} space can all be related to those at the 20 points in the $\frac{1}{48}$ th irreducible section of the Brillouin zone.

After the Fock matrix elements are evaluated with an initial estimate of $\underline{D}^{c'l}$, the secular equation (8) was solved at the selected set of \vec{k} values iteratively to a convergence limit of 0.001 in any density matrix element. Increasing the number of points leads to no significant change in the converged band structure.

A density-of-states histogram was constructed from solutions at the equivalent of 32768 points.

III. RESULTS

We describe first the computationally most accurate results obtained from the basis including Ti 1s through 3d and O 1s through 2p AO's with each Sr⁺² taken as a +2 point charge. Justifications for minimizing the significance of the Sr and higher-energy Ti AO's are deferred to Sec. IV.

Figures 3(c)-3(f) show graphs of $\epsilon(\nu\vec{k})$ vs \vec{k} , along the symmetry lines indicated in Fig. 2, for the upper occupied bands and the titanium 3d conduction band. Figure 4 contains the density-of-states histogram for energies above the Ti 3s valence band.³³ Values of the independent elements of the overlap and converged Fock and density matrices are contained in Table II; $q_{\text{Ti}} = +2.677$ and $q_{\text{O}} = -1.559$ at convergence, not too different from Kahn and Leyendecker's assumption.

Valence Bands

The valence 3s and 3p bands are narrow and lie well below the oxygen 2s and 2p bands. The 2s band has an appreciable width, mainly from 3d-2s interactions, and an ionization potential of 26 eV.

Most of the optical properties arise in transitions from the 2p valence bands, which differ in some detail from Kahn and Leyendecker's results. For example, our results interchange the two Γ_{15} levels at $\vec{k}=0$ and the Δ bands correlating with them. This may be attributed both to the significantly different O-O off-diagonal overlap and transfer integrals and to the "repulsive" effect of the Ti 3p AO's. Further, from investigations of the optical-absorption edge under stress and electric field, Casella suggests that the valence band ($\Gamma_{15} - \Delta_5 - X_5$) lies energetically above the other 2p valence bands.³ From symmetry he attributes the first direct interband transition probably from

Δ_5 to Δ'_2 . This result is in agreement with our ordering of the valence and conduction bands.

The ordering of these valence bands in Fig. 3 and the separation of these levels at $k=0$ are in agreement with Mattheiss's results for ReO₃.⁷ In fact the O-O interaction matrix elements, to which the 2p orbital splittings are very sensitive, should be very similar in these two compounds. In detail and in over-all width, however, the 2p valence band is also strongly influenced by 3d-2p interactions. Our over-all 2p band width is 5.9 eV compared to an earlier 3.6-eV measurement by soft-x-ray emission.^{33,34}

Since the Ti 3s and 3p AO's are usually regarded as inner-shell functions, a separate band-structure calculation was done, in which those functions were transferred to the frozen-core set. This change eliminates the constraint that the oxygen 2s and 2p bands be orthogonal to the Ti 3s and 3p and also leads to slightly different self-consistent charges on Ti and O. Comparing this to the previous result reveals a general lowering and broadening of the O 2p bands. Furthermore, individual band energies are shifted by as much as 7 eV, leading to a considerably different detailed structure in the diagram. For example, without explicit Ti 3s, 3p interactions, the highest part of the valence band shifts from Γ_{15} to the line $T_{1'}$. Our results thus indicate that the "inner-shell" Ti 3s and 3p AO's have considerable influence upon the valence orbital structure and must be included.

The reason for this influence is readily seen upon observing that the 3s and 3p AO's have a radial extension comparable to the 3d AO's and thus have comparable interactions with orbitals of neighboring ions. The Ti 1s, 2s, and 2p and O 1s AO's, however, are far more compactly localized about their respective nuclei. Two-center overlap distribution involving these AO's are very much smaller. Thus retaining them in the frozen core is a much more acceptable approximation.

Conduction Bands

Numerous investigations of the 3d conduction band structure of SrTiO₃ appear to agree with the features of the Kahn and Leyendecker model.¹ Their main conclusion is that the lowest conduction band is formed from the 3d t_{2g} AO's. It is flat along the cubic axes (so that the longitudinal effective mass m_l is infinite), since one component of the 3d t_{2g} set does not mix with any oxygen orbitals for values of \vec{k} along Δ . The conduction band rises in all other directions in \vec{k} space forming six degenerate ellipsoids with axes along the $\langle 100 \rangle$ directions in the Bravais lattice. The transverse effective mass m_t corresponding to the separation $X_3 - M_5$ is approximately equal to the free-electron mass.

Our results also agree with these features, though the LCAO Hartree-Fock calculation gives a larger over-all $3d$ -conduction-band width. The $3d$ - $2p$ covalency and overlap matrix elements which are mainly responsible for the conduction-band width are larger than those estimated by Kahn and Leyendecker. This is in agreement with a pre-

liminary result mentioned by Mattheiss for an APW calculation on SrTiO_3 .⁷ In particular, the X_3 - M_5 separation is 2.2 eV, corresponding to $m_i = 0.4m_0$.

Measurements of magnetoresistance are generally consistent with the conduction-electron energy surface.³⁵ However, they give an effective-mass

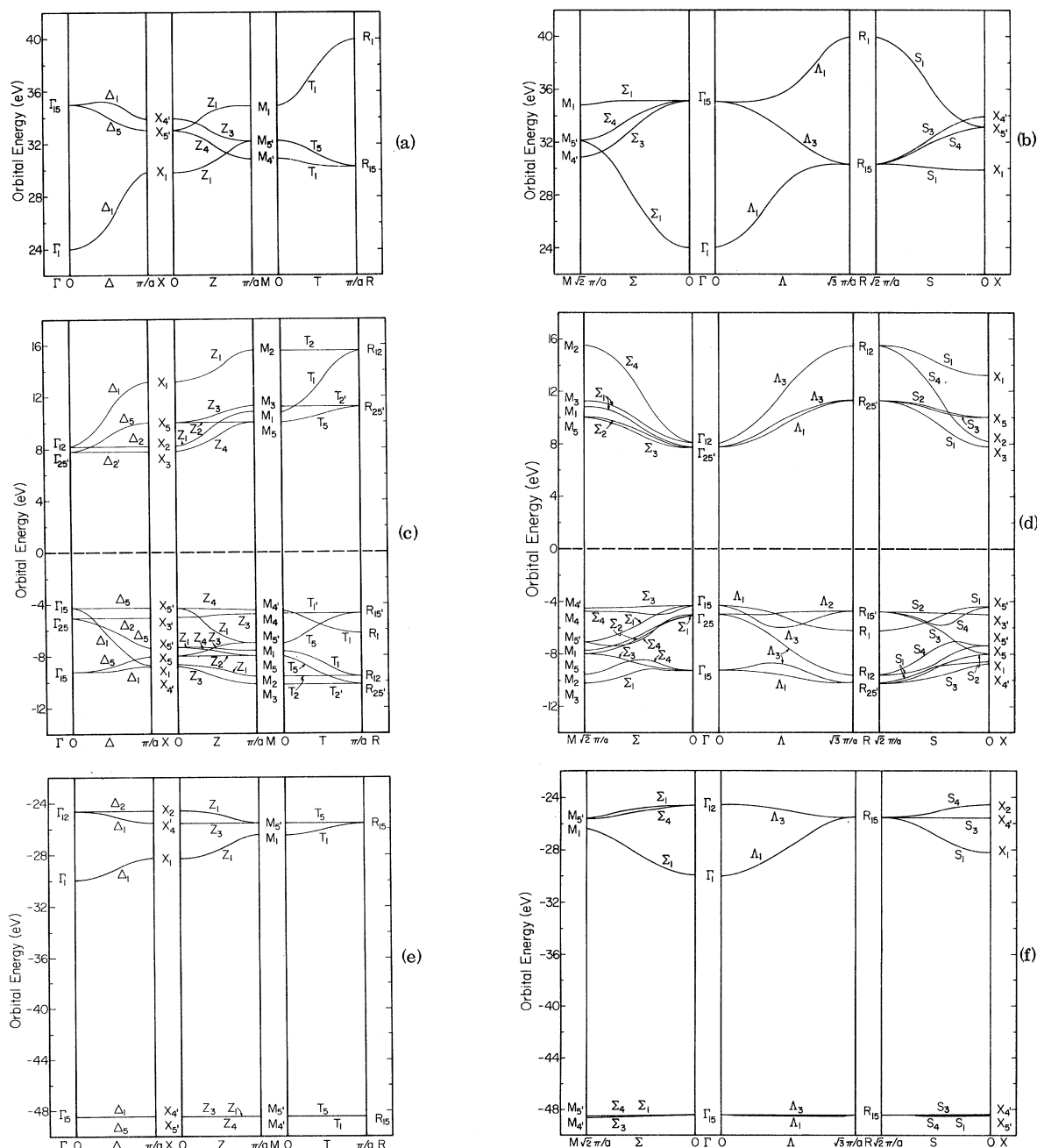


FIG. 3. Band orbital energies vs \vec{k} along symmetry lines in the Brillouin zone. Sections (c), (d), (e), and (f) show SCF results excluding the Ti $4s$ and $4p$ functions. Sections (a) and (b) show those additional bands, as obtained from the Hartree-Fock potential of the previous calculation.

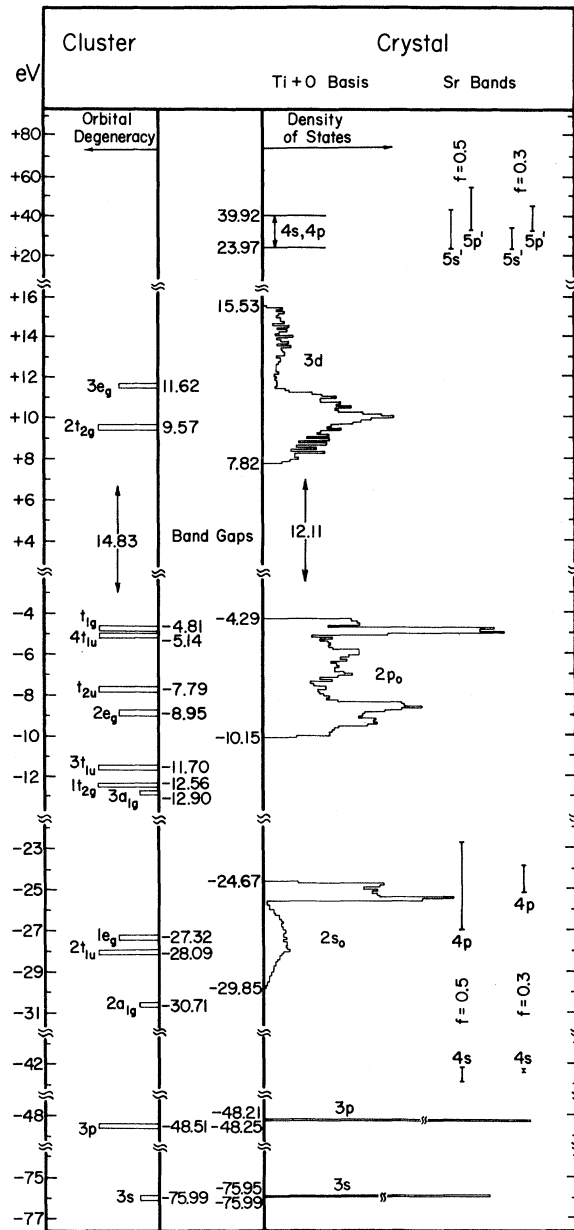


FIG. 4. Density-of-states histogram for SrTiO₃ and orbital-energy diagram for the TiO₆⁻⁸ cluster (Ref. 10). The latter energies have been shifted downward by 46.3 eV, approximately, to compensate for an extra-cluster Madelung potential. See text for discussion. Note change in energy scale above +16 eV. Numbers within the figure indicate extrema of bands or values of cluster ϵ 's. Only ranges are indicated for Ti 4s, 4p and Sr bands, obtained by the subsequent addition of those functions to the original basis.

anisotropy $K = m_l/m_t$ of around 4. Kahn and Leyendecker estimated $m_l = (20 \text{ to } 50)m_0$ from the inclusion of Ti-Ti overlap effects which caused Δ_2 to curve slightly downward giving a conduction-

band minimum at the zone edge. In Mattheiss's ReO₃ APW calculation however, Δ_2 curves 0.1 eV upward, giving a minimum at Γ .⁷ An accurate assessment of the Ti-Ti transfer elements is necessary to resolve this question here.

From our results the lowest-lying t_{2g} band is seen to lie only slightly below the lowest e_g band. Šroubek recently reconsidered the basic assumption that the t_{2g} band was the lowest conduction band.⁴ Based on estimated corrections to Kahn and Leyendecker's point-charge model, he proposed that the ordering of Γ_{12} and $\Gamma_{25'}$ might be inverted making the e_g band lower in energy. The difference between the diagonal matrix elements $E(3d_{xy}, 3d_{xy})$ and $E(3dz^2, 3dz^2)$ given in Table II supports Šroubek's result. However, the (3d-2s) covalency terms, which he was not able to evaluate, act to restore the order and qualitatively confirm the Phillip's³⁶ and Cohen and Heine³⁷ "cancellation theorem" invoked by Kahn and Leyendecker to justify using the point-ion approximation.

Band Gap

If SrTiO₃ does exhibit band-to-band transitions beginning at ~ 3.2 eV,¹⁴ the 12.1-eV gap obtained raises three major questions: (i) Is the computational methodology adequate? (ii) Does the Hartree-Fock model provide a useful basis to describe electronically excited states of crystals? (iii) Is an alternative interpretation of the spectrum required? We give some answers to (i) here and in Sec. IV and discuss (ii) and (iii) in Sec. V.

Two preliminary band-structure calculations were carried out using different oxygen bases, each having a single Slater-type orbital (STO) for each oxygen 2p AO, with orbital exponents $\zeta_{2p} = 1.8$ and 2.1. These band-structure results indicate that the widths of the valence and conduction bands are sensitive to that part of the basis but that the computed band gap is not. In addition, a calculation was made with the same basis but with empirical corrections so that those parts of the diagonal matrix elements which correspond to free-ion oxide ionization potentials agree with the values quoted by Kahn and Leyendecker.

Obtaining self-consistency in the charge distribution, however, does have a large effect on the band gap. As calculated from our AO basis, a classical, completely ionic structure ($q_{Ti} = +4$, $q_O = -2$) yields a 4.1-eV separation between an oxygen 2p π AO and the vacant 3de AO's (the 3d t_{2g} are 2.4 eV higher). The energy bands obtained from this initial field yield a 4.26-eV separation between Γ_{15} and $\Gamma_{25'}$, but also $q_{Ti} = +2.26$ and $q_O = -1.41$. Going into the next iteration of the SCF procedure with the latter Ti and O charge distributions, produces only a small lowering of the oxygen levels, but a large increase in $\Gamma_{15} - \Gamma_{25'}$ separation (to

TABLE III. Additional overlap and transfer integrals for the inclusion of titanium 4s and 4p AO's. [See Table II for definitions. $S(4s, 3s) = S(4px, 3px) = E(4s, 3s) = E(4px, 3px) = 0.$]

$\chi_I - \chi_{I'}$	$S(l, l')$	$E(l, l')$
4s -4s	1.0	0.185 68
-2s ₁	0.170 71	-0.197 71
-2px ₁	-0.225 92	0.128 54
4px-4px	1.0	0.535 10
-2s ₁	0.254 07	-0.260 00
-2px ₁	-0.293 47	0.100 32
-2px ₃	0.106 29	-0.057 26

14.8 eV) in large part for the reasons given by Šimánek and Šroubek in their criticism of Kahn and Leyendecker's approach. From this iteration $q_{Ti} = +2.88$ and $q_O = -1.63$. During iteration to convergence q_{Ti} , q_O , and the band gap oscillate slightly about the final values of +2.68, -1.56, and 12.1 eV, respectively.

While numerical approximations have been made, and some contributions to the exchange potential operator have been ignored, we are convinced after some investigation that no such factors could have caused the computed band gap to be four times too large. In the present calculation, any significant transfer of charge from oxygen to titanium must lead to a large 2p-3d band gap. We thus turn to possible influences of Ti 4s and 4p and of Sr AO's upon these results.

IV. EFFECTS OF ADDITIONAL Sr AND Ti AO's

Addition of Ti 4s, 4p AO's and explicit inclusion of Sr AO's introduces complications with respect to the capability of our present computer programs. *Free-ion* Ti 4s, 4p and Sr 5s, 5p AO's are very diffuse; non-nearest-neighbor overlap and transfer matrix elements involving them are large even at considerable separations and simply cannot be ignored. Furthermore, most integrals entering such transfer elements are very difficult to evaluate accurately within the present formalism. An alternative choice of basis, however, permits some semiquantitative conclusions to be drawn.

Alternative Basis

Given that *free-ion* valence and extra-valence shell AO's are yet to be found optimum for any molecular or crystal basis, we have simply designed variational functions for the crystal basis which suit the present computational requirements.

Like our oxide 2p function, the Ti 4s and 4p functions used were designed to represent behavior within the region of nearest neighbors, but to be negligibly small outside. After considerable investigation, the 6s and 6p STO's indicated in Table

I were chosen to represent the outer loops of the 4s and 4p AO's and orthogonalized to the previously determined 1s through 3p STO's. Outer maxima of the resulting 4s and 4p AO's come at $\sim 2 \text{ \AA}$ from the Ti nucleus; the basic nearest-neighbor Ti-Ti interaction integrals involving these functions are the order of 0.1 eV or smaller and, with reasonable safety, are neglected.

By exactly the same methods as described in Sec. II, the corresponding overlap and transfer elements given in Table III were evaluated using the density matrix given in Table II.

Two sets of functions are considered for Sr AO's. For one, atomic Sr-STO exponents³⁸ were used for inner shells and the exponents for the outermost shells were optimized with respect to total energy. For the other ("contracted"), the 5s' and 5p' AO functions incorporate the same 6s and 6p STO's used for Ti, but here orthogonalized to the Sr core orbitals. See Table I for details.

Diagonal transfer integrals involving Sr AO's were evaluated by the method outlined by Kahn and Leyendecker,¹ using our previously computed Ti and O charges for the Madelung-potential term. For band calculations using free-ion Sr AO's, experimental orbital energy (ionization potential) data were taken; using the contracted 5s', 5p' functions, the theoretical values were entered instead. See Table IV for numerical values.

Transfer integrals connecting Sr AO's to adjacent Ti, O, and Sr AO's were estimated by a modification of the Wolfsberg-Helmholz recipe²⁷:

$$E(\chi_{Sr}, \chi_I) \approx T(\chi_{Sr}, \chi_I) + \frac{1}{2} f S(\chi_{Sr}, \chi_I) [E(\chi_{Sr}, \chi_{Sr}) - T(\chi_{Sr}, \chi_{Sr}) + E(\chi_I, \chi_I) - T(\chi_I, \chi_I)] \quad (28)$$

where

TABLE IV. Sr atomic-orbital energies (eV).

Sr AO	Orbital energy	
	Calc ^a	Expt ^b
4s	-61.03	-61.4 ^c
4p	-40.84	-43.6
5s	-7.70	-11.03
5p	-6.19	-8.09
5s'	+5.09	-11.03
5p'	+13.29	-8.09

^aSCF orbital energies; 4s and 4p pertain to Sr⁺² and the others for Sr⁺¹ in the appropriate configuration.

^bAssembled from ionization potential and spectral data given by C. E. Moore, *Atomic Energy Levels*, Natl. Bur. Std. (U. S.), Circ. 467 (U. S. GPO, Washington, D. C., 1949).

^cEstimated by subtracting from the 4p ionization potential the difference in the Sr 4s and 4p x-ray atomic energy levels. [J. A. Beard and A. F. Burr, *Rev. Mod. Phys.* **39**, 125 (1967).]

$$T(\chi_{1'}, \chi_1) = \langle \chi_{1'} | -\frac{1}{2} \nabla^2 | \chi_1 \rangle.$$

Fitting the more accurately computed Ti-O transfer elements of Table II to Eq. (28) yields values of the adjustable parameter f mostly ranging from 0.3 to 0.5. Several band calculations using Sr functions were done for factors ranging between those limits. At the outset, it must be stated that Eq. (28) is completely undefended, from considerations of the Madelung-potential effects alone, when applied to the *free-ion* 5s and 5p functions. With them, at least second-nearest-neighbor Sr AO's must be included to prevent linear dependence when solving Eq. (8) for some values of \bar{k} .

Extended Band-Structure Results

Adding Ti 4s and 4p AO's makes little change in Figs. 3(c)-3(f) or in conclusions drawn from them. As shown in Figs. 3(a), 3(b), and 4, these bands lie well separated above the 3d band. Their inclusion does not change the band gap by more than ~ 0.2 eV.

Adding the Sr 4s and 4p AO's brings initial concern, since the latter come at the same energy range as the oxygen 2s bands. The spatial extent of the 4p's, however, is so restricted that there is little interaction between them and the 2s's. There simply is added essentially 4p band near the top of the existing 2s band, which increases its upward extent by a small amount depending upon the value chosen for f , as shown in Fig. 4. The Sr 4s and 4p's have a somewhat greater effect on the 2p valence bands. The bottom of these bands is raised by ~ 0.6 eV due to the (greater) upward shift of *lower* components such as M_3 and $R_{25'}$, which interact with those Sr AO's.

While solutions with Sr 5s and 5p are much less definitive, they do suggest some interesting aspects of the interactions of diffuse AO's in a crystal. With $f=0.3$, the *free-ion* 5s, 5p bands are extremely wide. They start below the 3d conduction band (at 10.7 eV above the top of the valence band) but do not seriously disrupt its main features. As f approaches 0.5, these bands are raised by 8 to 12 eV and their disruptive effect is still less. The "contracted" 5s', 5p' bands behave much like the Ti 4s, 4p bands and come in the same energy range as shown in Fig. 4.

This last observation is striking. The diagonal Fock energy elements for the free-ion 5s and 5p functions are 16 and 21 eV lower than those used for the contracted functions (Table IV). On the other hand, the centers of the *bands* arising from the free-ion functions range between 1 eV higher for 5s ($f=0.3$) and 8 eV higher for 5p ($f=0.5$), compared to the centers of the corresponding "contracted" bands. This large upward shift of the diffuse relative to the contacted AO bands arises directly from the various Sr-Sr interactions, which

are large for the free-ion AO's at all points in k space.

From these various considerations we locate the Sr 4s and 4p bands and conclude that neither they nor the other functions considered in this section have significant effects upon the valence band structure or the band gap.

V. DISCUSSION

Returning now to the implications of the large band gap reported in Sec. III, which has survived the preceding considerations, we examine the matter of calculating excitation energies from the ground-state Hartree-Fock solution.

According to the theory of Fowler,⁶ the Hartree-Fock band gap should be reduced by polarization effects which accompany the excitation of an electron from a filled valence band to an empty conduction band. The problem of including the effects of correlation has been discussed extensively in the literature. Electronic polarization or self-energy is largely inertialess and affects transport properties but little. In many treatments the main change due to correlation is to shift rigidly the conduction bands relative to the valence bands so that the band gap is lowered by as much as 5 eV or so. Since our purpose is to present a straight Hartree-Fock calculation, we have not introduced this sort of effect at this stage. Instead, we elaborate some properties of the independent TiO₆⁻⁸ cluster and develop relationships of them to the present SrTiO₃ crystal results.

Figure 4 shows the molecular-orbital (MO) energy-level diagram previously calculated for TiO₆⁻⁸ with the same basis as gave the results of Sec. III. [Note that the cluster energies have been shifted downward by 46.3 eV, in part to compensate for the extra-cluster Madelung potential at the Ti site (36.8 eV). This shift cannot be exactly defined, however, since the somewhat different values of q_{T1} and q_o obtained from the cluster SCF calculation (+2.64 and -1.77, respectively) are inconsistent with a crystal charge distribution having $q_{Sr} = +2$. (In the cluster $q_{T1} + 6q_o = -8$ and in the crystal $q_{T1} + 3q_o = -2$, by stoichiometry.) While q_{T1} for the two cases differs by only 0.04, q_o is 0.21 more negative in the cluster result. Thus, for example, in the cluster the "3s" AO's are more destabilized by the nearest oxygens by $\sim 6(0.21)/R(\text{Ti-O}) = 9.3$ eV. The cluster "oxygen" MO's are less affected by this difference.] In Fig. 4, the "3s" cluster MO is positioned to coincide exactly with the bottom of the crystal 3s band.

Except for the size of the band gap, our conduction- and valence-band density-of-states histograms are very similar to Mattheiss's adjusted ReO₃ results.⁷

With respect to energy, the cluster and crystal

Ti $3p$ states are very close. The centroids of the cluster O $2s$ and $2p$ states are somewhat lower and the latter are ~ 2 eV more widely spread. The cluster $3de_g$ and $3d t_{2g}$ MO's fall in the lower portion of the crystal conduction band. The cluster "band gap" is 2.3 eV greater than that of the crystal.

Particularly striking is the additional similarity in density of states. Five of the six oxygen $2s$ MO's occur near the top of that range just as the crystal density-of-states histogram is very large there. Likewise, the pattern of oxygen $2p$ MO's appears also in the $2p$ valence band. The maximum in the conduction band is but $\frac{1}{2}$ eV higher than the position of the $3dt_{2g}$ MO's and 78% of its states lie below the energy of the $3de_g$ MO's. The weighted averages of the crystal and cluster "3d" states are 10.3 and 10.4 eV, respectively, which is to be expected if the adjustment of the cluster MO energies is valid and if the cluster $3d$ MO's were actually to represent Wannier functions for the crystal.³⁹ In such event, Mattheiss⁸ has shown further that second-order perturbation theory predicts that the difference in average energies of the de_g and dt_{2g} bands should equal the difference ($10Dq$ in crystal field theory) in the energies of the de_g and dt_{2g} Wannier functions. That is,

$$10Dq \approx E(3dz^2 - 3dz^2) - E(3dxy - 3dxy) + \frac{1}{2}(\Delta_s + \Delta_\sigma - \Delta_\pi), \quad (29)$$

where

$$\begin{aligned} \Delta_s &= E(\Gamma_{12}) - E(3dz^2 - 3dz^2), \\ \Delta_\sigma &= E(R_{12}) - E(3dz^2 - 3dz^2), \\ \Delta_\pi &= E(R_{25'}) - E(3dxy - 3dxy). \end{aligned}$$

From our band results, Eq. (29) yields $10Dq = 2.27$ eV compared to the cluster value + 2.05 eV.

The notable similarities in energy-level distribution suggest that the total band structure may well contain significant characteristics of the cluster unit. We consider next the calculations of actual electronic excitation energies.

Charge-Transfer Transitions in the TiO_6^{-8} Cluster

In the TiO_6^{-8} cluster, the lowest electronic transitions are of the charge transfer type and occur from oxygen $2p\pi$ MO's to the vacant titanium t_{2g} and e_g orbitals. We illustrate the computation of the excitation energy to an average of states arising from the spatially allowed $4t_{1u} \rightarrow 2t_{2g}$ (i.e., $2p\pi_O \rightarrow 3dt_{2g}$) transitions.^{10, 21}

The orbital energy difference, $\epsilon(2t_{2g}) - \epsilon(4t_{1u})$, equals 14.7 eV. The excitation energy, however, is lowered by the electron-hole interaction. Using Koopmans's theorem,²⁵ which assumes there is no electronic reorganization in going from the ground to the first excited state,

$$\Delta E \approx \epsilon(2t_{2g}) - \epsilon(4t_{1u}) - \bar{J}(2t_{2g}, 4t_{1u}). \quad (30)$$

The Coulomb interaction \bar{J} is computed to be 7.9 eV, slightly greater than the point-ion estimate $e^2/R(\text{Ti-O}) = 7.3$ eV. Very much smaller exchange interactions, ~ 0.06 eV, separate the sets of singlet and triplet excited states. Hence, using Koopmans's theorem, $\Delta E \approx 6.8$ eV.

The same excited-state energy was also computed using the Hartree-Fock-Roothaan open-shell SCF procedure developed for octahedral transition-metal clusters.²¹ This calculation gives $\Delta E = 4.2$ eV above the ground state. That is, an additional 2.7 eV is gained when the excited state is computed independently and is attributed to electronic reorganization upon excitation.

Implications for SrTiO_3

Just as the cluster model for binary and ternary ionic transition-metal salts yields good energy values for the $d-d$ transitions, it also appears to yield a good estimate for the onset of charge transfer excitations observed in this system. That model is fully consistent with these crystal results, however, *only if* the actual transitions are not *band to band* but rather if the hole and particle are correlated in the excited state. This is essentially the situation postulated by Šimánek and Šroubek.⁵ Such correlation may be introduced if the electronically excited crystal states Φ_λ are represented more accurately by a superposition of all vertical band-to-band promotions (configuration interaction)

$$\Phi_\lambda = \sum_{b,B} \sum_{\vec{k}} c_{\lambda}(bB, \vec{k}) \Psi(bB, \vec{k}), \quad (31)$$

where $\Psi(bB, \vec{k})$ is a wave function constructed from the manifold of ground-state SCF band orbital functions in which one electron is promoted from a ground-state-occupied band b to a conduction band B both at \vec{k} .

The expansion in Eq. (31) is just the fundamental starting point in the construction of excitonic states. In a subsequent paper, we shall show that hole-particle excitation states can indeed be constructed from the present results in this manner and that they exhibit orbital and energy features very similar to the charge-transfer excited states of the TiO_6 cluster unit. In this respect, SrTiO_3 has the characteristics of a molecular crystal composed of (linked) TiO_6 units.

Relative to the ground state of the crystal, the energy of the state Φ_λ may be written in the form

$$\Delta E_\lambda = \langle \Delta \epsilon \rangle_\lambda - E_{hp\lambda} - \Delta E_{p\lambda}, \quad (32)$$

where $\langle \Delta \epsilon \rangle_\lambda$ is the appropriate averaged occupied-to-vacant-band energy difference. We find that values of the hole-particle interaction energy $E_{hp\lambda}$ are close to values of the analogous Coulomb in-

tegrals which occur in applying Eq. (30) to the cluster but that values of $\langle \Delta\epsilon \rangle_\lambda$ begin at about 16 eV, roughly 2 eV higher. Regarded as electronic polarization energy, or reorganization energy for the excited state of the crystal, $\Delta E_{P\lambda}$ may reasonably be expected to exceed the value of 2.7 eV determined in the isolated cluster calculation. The classical electrostatic calculation of Šimánek and Šroubek, in fact, would place it at ~ 6 eV.⁵ Using *this* value and following the above reasoning, the present band structure results are then found to predict (excitonic) states beginning at about 2 eV and extending up towards the 12.1-eV direct band gap.

Such a prediction of excitonic lower-excited states would appear to conflict with the photoconductivity observed when the crystal is irradiated at ~ 3 eV.⁴⁰ Mechanisms have been postulated, however, to account for such phenomena. These and other processes are discussed in a subsequent paper.

VI. SUMMARY

It appears both possible and worthwhile to compute the energy bands of an insulating crystal like SrTiO₃ using the SCF tight-binding method. Instead of employing pseudopotentials or Fourier expansions of the crystal potential, we explicitly evaluated all the integrals appearing in the tight-binding formalism which are associated with a cluster of nearest-neighbor atoms. Since it has been shown that different model potentials can yield appreciably different positions and characters of energy bands, it is imperative that detailed calculations like this be performed in order to understand the limits of the Hartree-Fock approxima-

tion.

Encouragingly good agreement is obtained with experiment both as regards the relative ordering of the energy bands and the determination of transport properties. As further data from x-ray-absorption and -emission and electron-emission spectroscopy become available, it will be possible to check the absolute positions of the one-electron energy bands.

This LCAO-Hartree-Fock calculation yields a separation between the lowest filled oxygen *2p* bands and the vacant titanium *3d* bands of 12 eV. While this is much larger than the observed optical-absorption edge at 3.2 eV, we expect that many electron effects are very important in the optically excited state of the crystal. A consideration of configuration interaction between band-to-band excited configurations and an estimate of polarization effects suggests that these correlation terms will reduce the band gap by the right amount.

Finally, we have shown that achieving a self-consistent charge distribution is very important in determining the band gap of these ionic materials.

ACKNOWLEDGMENTS

The authors wish to thank Professor J. M. Honig for bringing this problem to their attention and to express their deep appreciation to him for continuing encouragement and helpful discussion throughout this work. We also are much indebted to Dr. P. M. Castle for his cooperation in supplying the basic TiO₆ data and his results. One of us (J. W. R.) is deeply grateful for the hospitality accorded him in Professor Polder's group at the Philips Research Laboratories where much of the fundamental analysis was done.

*Work supported in part by Contract SD-102 with the Advanced Research Projects Agency. Based in part upon the doctoral dissertations of T. F. Soules and E. J. Kelly.

†Present address: Lighting Research Laboratory, General Electric Company, Cleveland, Ohio 44112.

‡Present address: Chemistry Department, Memphis State University, Memphis, Tenn. 38111.

¹A. H. Kahn and A. J. Leyendecker, Phys. Rev. **135**, A1321 (1964).

²H. P. R. Frederikse, W. R. Hosler, and W. R. Thurber, J. Phys. Soc. Japan Suppl. **21**, 32 (1966); H. P. R. Frederikse, in *Electronic Structures in Solids*, edited by E. D. Haidemenakis (Plenum, New York, 1969).

³R. C. Casella, Phys. Rev. **154**, 743 (1967).

⁴Z. Šroubek, Phys. Rev. B **2**, 3170 (1970).

⁵E. Šimánek and Z. Šroubek, Phys. Status Solidi **8**, K47 (1965).

⁶W. B. Fowler, Phys. Rev. **151**, 657 (1966).

⁷L. F. Mattheiss, Phys. Rev. **181**, 987 (1969).

⁸L. F. Mattheiss, Phys. Rev. B **2**, 3918 (1970).

⁹T. F. Soules, J. W. Richardson, and D. M. Vaught,

Phys. Rev. B **3**, 2186 (1971); J. W. Richardson, D. M. Vaught, T. F. Soules, and R. R. Powell, J. Chem. Phys. **50**, 3633 (1969).

¹⁰J. W. Richardson and P. M. Castle (unpublished).

¹¹For a comparison of results obtained for alkali halides using various (crystal) exchange potentials see A. B. Kunz, W. B. Fowler, and P. M. Schneider, Phys. Letters **28A**, 553 (1969).

¹²See N. O. Lipari and A. B. Kunz, Phys. Rev. B **4**, 4639 (1971), and references to other work cited therein.

¹³More recently, other computational methods have been advanced which deal, at least in part, with the apparent overestimation of excitation energies by applying the normal Hartree-Fock calculation to the general state. In particular should be noted the $X\alpha$ self-consistent-field method; see J. C. Slater, in *Computational Methods in Band Theory*, edited by P. M. Marcus, J. F. Janak, and A. R. Williams (Academic, New York, 1971). W. A. Goddard, III and P. M. O'Keefe, in the same volume, describe some others also.

¹⁴M. Cardona, Phys. Rev. **140**, A651 (1965). See also: M. I. Cohen and R. F. Blunt, *ibid.* **168**, 929 (1968); W. S. Baer, J. Phys. Chem. Solids **28**, 677 (1967);

- M. Capizzi and A. Frova, *Phys. Rev. Letters* **25**, 1298 (1970); Y. T. Sihvonen, *J. Appl. Phys.* **38**, 4431 (1967).
- ¹⁵E. E. Lafon and C. C. Lin, *Phys. Rev.* **152**, 579 (1966).
- ¹⁶R. C. Chaney, C. C. Lin, and E. E. Lafon, *Phys. Rev. B* **3**, 459 (1971).
- ¹⁷J. M. Tyler and J. L. Fry, *Phys. Rev. B* **1**, 4604 (1970).
- ¹⁸J. M. Tyler, T. E. Norwood, and J. L. Fry, *Phys. Rev. B* **1**, 297 (1970).
- ¹⁹T. E. Norwood and J. L. Fry, *Phys. Rev. B* **2**, 472 (1970).
- ²⁰L. B. Bouckaert, R. Smoluchowski, and E. Wigner, *Phys. Rev.* **50**, 58 (1936).
- ²¹J. W. Richardson, T. F. Soules, D. M. Vaught, and R. R. Powell, *Phys. Rev. B* **4**, 1721 (1971).
- ²²J. W. Richardson, W. C. Nieuwpoort, R. R. Powell, and W. F. Edgell, *J. Chem. Phys.* **36**, 1057 (1962); J. W. Richardson, R. R. Powell, and W. C. Nieuwpoort, *ibid.* **38**, 796 (1963).
- ²³S. Nagai, *J. Phys. Soc. Japan* **22**, 457 (1967).
- ²⁴R. E. Watson, *Phys. Rev.* **111**, 1108 (1958).
- ²⁵C. C. J. Roothaan, *Rev. Mod. Phys.* **23**, 69 (1951); C. C. J. Roothaan and P. Bagus, *Methods in Computational Physics* (Academic, New York, 1963), Vol. II, pp. 47-94.
- ²⁶J. M. Honig, J. O. Dimmock, and W. H. Kleiner, *J. Chem. Phys.* **50**, 5232 (1969).
- ²⁷M. Wolfsberg and L. Helmholz, *J. Chem. Phys.* **20**, 837 (1952).
- ²⁸F. Michel-Calendini and M. G. Mesnard, *Phys. Status Solidi* **B44**, K117 (1971).
- ²⁹R. S. Mulliken, *J. Chem. Phys.* **23**, 1833 (1955).
- ³⁰See also S. Sugano and R. G. Shulman, *Phys. Rev.* **130**, 517 (1963).
- ³¹Y. Sakamoto and U. Takahasi, *J. Chem. Phys.* **30**, 337 (1959).
- ³²R. S. Mulliken, *J. Chim. Phys.* **46**, 497 (1949).
- ³³Comparison of the absolute values of the band energies to known x-ray ionization energies and recent electron spectroscopy for chemical analysis (ESCA) results is deferred to a subsequent note.
- ³⁴M. A. Blokhin and A. T. Shuvaev, *Bull. Acad. Sci. USSR, Phys. Ser.* **26**, 429 (1962).
- ³⁵H. P. R. Frederikse, W. R. Hosler, and W. R. Thurber, *Phys. Rev.* **143**, 648 (1966); O. N. Tutte and E. L. Stelzer, *ibid.* **173**, 775 (1968); H. P. R. Frederikse, W. R. Hosler, W. R. Thurber, J. Babiskin, and P. G. Siebenmann, *ibid.* **158**, 775 (1967).
- ³⁶J. C. Phillips, *J. Phys. Chem. Solids* **11**, 226 (1961).
- ³⁷M. H. Cohen and V. Heine, *Phys. Rev.* **122**, 1821 (1961).
- ³⁸E. Clementi, D. L. Raimondi, and W. P. Reinhardt, *J. Chem. Phys.* **47**, 1300 (1967).
- ³⁹P. W. Anderson, in *Solid State Physics*, edited by F. Seitz and D. Turnbull (Academic, New York, 1963), Vol. 14.
- ⁴⁰L. Grabner, *Phys. Rev.* **177**, 1315 (1969).

Second-Sound Velocities in Cubic Crystals*

Y. P. Varshni and A. Konti

Department of Physics, University of Ottawa, Ottawa, Canada K1N 6N5

(Received 10 April 1972)

Accurate values of "drifting" and "driftless" second sound at 0 K are obtained for alkali-halide crystals and ten other cubic crystals. The percentage difference between the two types of second sound is found to vary from 3.8 to 16.2%. The ratio $R = \langle v^2 \rangle / 3v_{II}^2$, where v is the sound velocity and v_{II} is the drifting second-sound velocity, is also studied and is shown to be correlated with the degree of anisotropy of the substance.

I. INTRODUCTION

At low temperatures the study of heat pulses yields valuable information concerning the phonon-scattering process in dielectric crystals. The possibility of the existence of a propagating temperature wave, called second sound, in a solid was first suggested by Peshkov.¹ Later Ward and Wilks^{2,3} showed that it is theoretically possible for a temperature pulse to propagate through a phonon gas in a wavelike form, and they predicted the following relation between the second-sound velocity v_{II} and the mean sound velocity c :

$$v_{II}^2 = \frac{1}{3}c^2 \quad (1)$$

Since that time considerable effort has gone into establishing theories⁴ of a more fundamental nature providing a more rigorous justification for the existence of second sound in insulators. Enz⁴ has shown that two types of second sound are possible: "drifting" and "driftless."

In recent years a number of observations on heat-pulse propagation in solids with characteristics associated with the "second sound" have been made. In 1966, Ackermann *et al.*⁵ were the first to observe second sound in solid ⁴He. Subsequently, more attempts were made by others with varying degrees of success and recently heat-pulse data and observations of second sound in very pure